International Journal on New Computer Architectures and Their Applications (IJNCAA) 1(1): 1-14
The Society of Digital Information and Wireless Communications, 2011 (ISSN: 2220-9085)

Assessment Procedure of the EM Interaction between Mobile Phone Antennae and Human Body

Salah I. Al-Mously
School of Computer Engineering, Koya University, Koya, Erbil, Iraq
salah.mously@ieee.org

ABSTRACT

This paper presents a procedure for the evaluation of the Electromagnetic (EM) interaction between the mobile phone antenna and human body, i.e., head and hand, and investigates the factors may influence this interaction. These factors are considered for different mobile phone handset models, different form factors and different antenna types, operating in the GSM900, GSM1800/DCS, and UMTS/IMT-2000 bands. A realistic usage of mobile phone handset next to head at *cheek* and *tilt* positions, in compliance with IEEE-standard 152, is considered during computations. Homogeneous and heterogeneous CAD-models are used to simulate the mobile phone user's head, whereas, a homogeneous model with three different tissues is designed to simulate the user's hand-hold. A validation of our EM interaction computation using both Yee-FDTD and ADI-FDTD is achieved by comparison with previously published works.

KEYWORDS

Dosimetry, FDTD, mobile phone antenna, MRI, phantom, SAM, specific absorption rate (SAR).

1 INTRODUCTION

Realistic usage of mobile phone handsets in different patterns imposes an EM wave interaction between the handset antenna and the human body (head and hand). This EM interaction due to the presence of the user's head close to the handheld set can be looked at from two different points of view; Firstly, the mobile handset has an impact on the user, which is often understood as the exposure of the user to the EM field of the radiating device. The absorption of electromagnetic energy generated by mobile handset in the human tissue, SAR, has become a point of critical public discussion due to the possible health risks. SAR, therefore, becomes an important performance parameter for the marketing of cellular mobile phones and underlines the interest in optimizing the interaction between the handset and the user by both consumers and mobile phone manufacturers.

Secondly, and from a more technical point of view, the user has an impact on the mobile handset. The tissue of the user represents a large dielectric and lossy material distribution in the near field of a radiator. It is obvious, therefore, that all antenna parameters, such as impedance, radiation characteristic, radiation efficiency and total isotropic sensitivity (TIS), will be affected by the properties of the tissue. Moreover, the effect can differ with respect to the individual habits of the user in placing his hand around the mobile handset or attaching the handset to the head. Optimized user interaction, therefore, becomes a technical performance parameter of cellular mobile phones.

The EM interaction of the cellular handset and a human can be evaluated using either experimental measurements or numerical computations, e.g., FDTD method. Experimental measurements make use of the actual mobile phone, but with a simple homogeneous human head model having two or three tissues. Numerical computation makes use of an MRI-based heterogeneous anatomically correct human head model with more than thirty different tissues, but the handset is modeled as a simple box with an antenna. Numerical computation of the EM interaction can be enhanced by using semi- or complete-realistic handset models [1]-[3]. In this paper, a FDTD method is used to evaluate the EM interaction, where different human head models, i.e., homogeneous and heterogeneous, and different handset models, i.e., simple and semi-realistic, are used in computations [4]-[12].

2 SPECIFIC ABSORPTION RATE (SAR)

It is generally accepted that SAR is the most appropriate metric for determining electromagnetic energy (EME) exposure in the very near field of a RF source [13]-[21]. SAR is expressed in watts per kilogram (W/kg) of biological tissue, and is generally quoted as a figure averaged over a volume corresponding to either 1 g or 10 g of body tissue. The SAR of a wireless product can be measured in two ways. It can be measured directly using body phantoms, robot arms, and associated test equipment (Fig. 1), or by mathematical modeling. The latter can be costly, and can take as long as several hours. The concept of correlating the absorption mechanism of a biological tissue with the basic antenna parameters (e.g., input impedance, current, etc.) has been presented in many papers, Kuster [22], for example, described an approximation formula that provides a correlation of the peak SAR with the square of the incident magnetic field and consequently with the antenna current.

(a) (b)

Figure 1. Different SAR measurement setups: (a) SAR measurement setup by IndexSAR company, http://www.indexsar.com, and (b) SAR measurement setup (DASY5) by SPEAG, http://www.speag.com.

Using the FDTD method, the electric fields are calculated at the voxel edges, and consequently, the *x*, *y*, and *z*-directed power components associated with a voxel are defined in different spatial locations. These components must be combined to calculate SAR in the voxel. There are three possible approaches to calculate the SAR: the 3-, 6-, and 12-field components approaches. The 12-field components approach is the most complicated but it is also the most accurate and the most appropriate from the mathematical point of view [23]. It correctly places all E-field components in the center of the voxel using linear interpolation. The power distribution is, therefore, now defined at the same location as the tissue mass. For these reasons, the 12-field components approach is preferred by IEEE-Std. 1529 [24].

The specific absorption rate is defined as:

$$SAR = \frac{\sigma_E}{2\rho} |\mathbf{E}|^2 = c\frac{dT}{dt} \qquad (1)$$

where c is the specific heat capacity, σ_E the electric conductivity, ρ the mass density of the tissue, $\mathbf{E}$ the induced electric field vector and dT/dt the temperature increase in the tissue.

Based on SCC-34, SC-2, WG-2 - Computational Dosimetry, IEEE-Std. 1529 [24], an algorithm has been implemented using a FDTD-based EM simulator, SEMCAD X [25], where for body tissues, the spatial-peak SAR should be evaluated in cubical volumes that contain a mass that is within 5% of the required mass. The cubical volume centered at each location should be expanded in all directions until the desired value for the mass is reached, with no surface boundaries of the averaging volume extending beyond the outermost surface of the considered region of the model. In addition, the cubical volume should not consist of more than 10% air. If these conditions are not met, then the center of the averaging volume is moved to the next location. Otherwise, the exact size of the final sampling cube is found using an inverse polynomial approximation algorithm, leading to very accurate results.

3 SAR MEASUREMENT AND COMPUTATION PROTOCOL

RF human exposure guidelines and evaluation methods differentiate between portable and mobile devices according to their proximity to exposed persons. Devices used in close proximity to the human body are evaluated against SAR limits. Devices used not close to the human body, can be evaluated with respect to Reference Levels or Maximum Permissible Exposure (MPE) limits for power density. When a product requires evaluation against SAR limits, the SAR evaluation must be performed using the guidelines and procedures prescribed by the applicable standard and regulation. While the requirements are similar from country to country, significant differences exist in the scope of the SAR regulations, the measurement standards and the approval requirements.
IEEE-Std. 1528 [13], EN 50360 [16] and EN 50361 [17], which replaced with the standard IEC 62209-1 [18], specify protocols and procedures for the measurement of the spatial-peak SAR induced inside a simplified model of the head of the users of mobile phone handsets. Both IEEE and IEC standards provide regulatory agencies with international consensus standards as a reference for accurate compliance testing.

The simplified physical model (phantom) of the human head specified in IEEE-Std. 1528 and IEC 62209-1 is the SAM. SAM has also been adopted by the European Committee for Electrotechnical Standardization (CENELEC) [16], the Association of Radio Industries and Businesses in Japan [19], and the Federal Communications Commission (FCC) in the USA [20]. SAM is based on the 90th percentile of a survey of American male military service personnel and represents a large male head, and was developed by the IEEE Standards Coordinating Committee 34, Subcommittee 2, Working Group 1 (SCC34/SC2/WG1) as a lossless plastic shell and an ear spacer. The SAM shell is filled with homogeneous fluid having the electrical properties of head tissue at the test frequency. The electrical properties of the fluid were based on calculations to give conservative spatial-peak SAR values averaged over 1 and 10 g for the test frequencies [26]. The electrical properties are defined in [13] and [27], with shell and ear spacer defined in [26]. The CAD files defining SAM show specific reference points and lines to be used to position mobile phones for the two compliance test positions specified in [13] and [26]. These are the *cheek*-position shown in Fig. 2(a) and the *tilt*-position shown in Fig. 2(b).

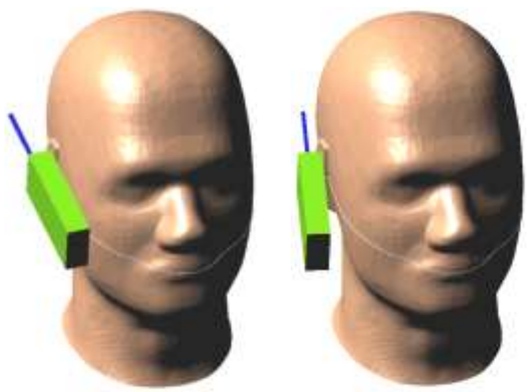

(a) (b)

Figure 2. SAM next to the generic phone at: (a) *cheek*-position, and (b) *tilt*-position in compliance with IEEE-Std. 1528-2003 [13] and as in [26].

To ensure the protection of the public and workers from exposure to RF EM radiation, most countries have regulations which limit the exposure of persons to RF fields from RF transmitters operated in close proximity to the human body. Several organizations have set exposure limits for acceptable RF safety via SAR levels. The International Commission on Non-Ionizing Radiation Protection (ICNIRP) was launched as an independent commission in May 1992. This group publishes guidelines and recommendations related to human RF exposure [28].

4 SAR EXPOSURE LIMITS

For the American National Standards Institute (ANSI), the RF safety sections now operate as part of the Institute of Electrical and Electronic Engineers (IEEE). IEEE wrote the most important publications for SAR test methods [13] and the standard safety levels [15].

The European standard EN 50360 specifies the SAR limits [16]. The limits are defined for exposure of the whole body, partial body (e.g., head and trunk), and hands, feet, wrists, and ankles. SAR limits are based on whole-body exposure levels of 0.08 W/kg. Limits are less stringent for exposure to hands, wrists, feet, and ankles. There are also considerable problems with the practicalities of measuring SAR in such body areas, because they are not normally modeled. In practice, measurements are made against a flat phantom, providing a conservative result.

Most SAR testing concerns exposure to the head. For Europe, the current limit is 2 W/kg for 10-g volume-averaged SAR. For the United States and a number of other countries, the limit is 1.6 W/kg for 1-g volume-averaged SAR. The lower U.S. limit is more stringent because it is volume-averaged over a smaller amount of tissue. Canada, South Korea and Bolivia have adopted the more-stringent U.S. limits of 1.6 W/kg for 1-g volume-averaged SAR. Australia, Japan and New Zealand have adopted 2 W/kg for 10-g volume-averaged SAR, as used in Europe [29]. Table 1 lists the SAR limits for the non-occupational users recommended in different countries and regions.

When comparing published results of the numerical dosimetric of SAR that is induced in head tissue due to the RF emission of mobile phone handsets, it is important to mention if the SAR values are based on averaging volumes that included or excluded the pinna. Inclusion versus exclusion of the pinna from the 1- and 10-g SAR averaging volumes is the most significant cause of discrepancies [26].

INCIRP Guidelines [28] apply the same spatial-peak SAR limits for the pinna and the head, whereas the draft IEEE-Std. C95.1b-2004, which were published later in 2005 [30], apply the spatial-peak SAR limits for the extremities to the pinnae (4 W/kg per 10-g mass rather than the 1.6 W/kg per 1g for the head). Some investigators [31], [32], treated the pinna in accordance with ICNIRP Guidelines, whereas others [33], [34], treated the pinna in accordance with the IEEE-Std. C95.1b-2004. For the heterogeneous head model with pressed air that was used in [4], [6], [9], [10] and [12], the pinna was treated in accordance with ICNIRP Guidelines.

Table 1. SAR limits for non-occupational/unaware users in different countries and regions.

	USA	**Europe**	**Australia**	**Japan**
Organization/Body	IEEE/ANSI/ FCC	ICNIRP	ASA	TTC/MPTC
Measurement method	C95.1	EN50360	ARPANSA	ARIB
Whole body averaged SAR	0.08 W/kg	0.08 W/kg	0.08 W/kg	0.04 W/kg
Spatial-peak SAR in head	1.6 W/kg	2 W/kg	2 W/kg	2 W/kg
Averaging mass	1 g	10 g	10 g	10 g
Spatial-peak SAR in limbs	4 W/kg	4 W/kg	4 W/kg	4 W/kg
Averaging mass	10 g	10 g	10 g	10 g
Averaging time	30 min	6 min	6 min	6 min

5 ASSESSMENT PROCEDURE OF THE EM INTERACTION

Assessment of the EM interaction of cellular handsets and a human has been investigated by many authors since the launch of second-generation systems in 1991. Different numerical methods, different human head models, different cellular handset models, different hand models, and different standard and non-standard usage patterns have been used in computations. Thus, varying results have been obtained. The causes of discrepancies in computations have been well investigated [26], [35]. Fig. 3 shows a block diagram of the proposed numerical computation procedure of both SAR induced in tissues and the antenna performance due to the EM interaction of realistic usage of a cellular handset using a FDTD method.

Assessment accuracy of the EM interaction depends on the following:

(a) *Mobile phone handset modeling.* This includes handset model (i.e., Dipole antenna, external antenna over a metal box, internal antenna integrated into a dielectric box, semi-realistic CAD model, and realistic *ProEngineer* CAD-based mode [3]), handset type (e.g., bar, clamshell, flip, swivel and slide), handset size, antenna type (e.g., whip, helix, PIF and MPA), and antenna position.

(b) *Human head modeling* (i.e., homogeneous phantoms including SAM, and heterogeneous MRI-based anatomically correct model). For the heterogeneous head model, the number of tissues, resolution, pinna thickness (pressed and non-pressed), and tissue parameters definition, all playing an important role in computing the EM interaction

(c) *Human hand modeling* (i.e., simple block, homogeneous CAD model, MRI-based model)

(d) *Positioning of handset, head and hand*. In the IEEE-Std. 1528-2003 [13], two handset positions with respect to head are adopted, *cheek* and *tilt*, but the hand position in not defined.

(e) *Electrical properties definition of the handset material and human tissues*.

(f) *Numerical method* (e.g., FDTD, FE, MoM, and hybrid methods). Applying the FDTD method, the grid-cell resolution and ABC should be specified in accordance with the available hardware for computation. Higher resolution and higher ABC needs a faster CPU and larger memory.

6 VALIDATIONS OF THE NUMERICAL DOSIMETRIC OF SAR

Verification of our FDTD computation was performed by comparison with the numerical and practical dosimetric given in [26], where the spatial-peak SAR over 1g and 10g induced in SAM is computed due to the RF emission of a generic phone at 835 and 1900 MHz normalized to 1 W source power. Both Yee-FDTD and ADI-FDTD methods were applied for the numerical computation using SEMCAD X [25] and compared with the results presented in [26].

As described in [26], the generic mobile phone was formed by a monopole antenna and a chassis, with the excitation point at the base of the antenna. The antenna length was 71 mm for 835 MHz and 36 mm for 1900 MHz, and its square cross section had a 1-mm edge. The monopole was coated with 1 mm thick plastic having dielectric properties $\varepsilon_r = 2.5$ and $\sigma = 0.005$ S/m. The chassis comprised a PCB, having lateral dimensions of 40 × 100 mm and a thickness of 1 mm, symmetrically embedded in a solid plastic case with dielectric properties $\varepsilon_r = 4$ and $\sigma = 0.04$ S/m, lateral dimensions 42× 102 mm, and thickness 21 mm. The antenna was mounted along the chassis centerline so as to avoid differences between right- and left-side head exposure. The antenna was a thick-wire model whose excitation was a 50-Ω sinusoidal voltage source at the gap between the antenna and PCB. Fig. 2 shows the generic phone in close proximity to a SAM phantom at *cheek* and *tilt*-position in compliance with IEEE-Std. 1528-2003 [13].

The simulation platform SEMCAD X incorporates automated heterogeneous grid generation, which automatically adapts the mesh to a specific setup. To align the simulated handset components to the FDTD grid accurately a minimum spatial resolution of 0.5×0.5×0.5 mm^3 and a maximum spatial resolution of 3× 3×3 mm^3 in the *x*, *y*, and *z* directions was chosen for simulating the handset in hand close to head. A refining factor of 10 with a grading ratio of 1.2 was used for the solid regions during the simulations. The simulations assumed a steady state voltage at 835 and 1900 MHz, with a feed point of 50-Ω sinusoidal voltage source and a 1 mm physical gap between the antenna and the printed circuit board. The ABCs were set as a UPML-mode with 10 layers thickness, where the minimum level of absorption at the outer boundary was > 99.9% [25]. Table 2 explains the amount of the FDTD-grid cells needed to model the handset in close proximity to SAM at 835 and 1900 MHz, according to the setting parameters and values mentioned above.

The FDTD computation results, using both Yee-FDTD and ADI-FDTD methods, are shown in Table 3. The computed spatial-peak SAR over 1 and 10g was normalized to 1 W net input power as in [26], at both 835 and 1900 MHz, for comparison. The computation and measurement results in [26], shown in Table 3, were considered for sixteen participants where the mean and standard deviation of the SARs are presented.

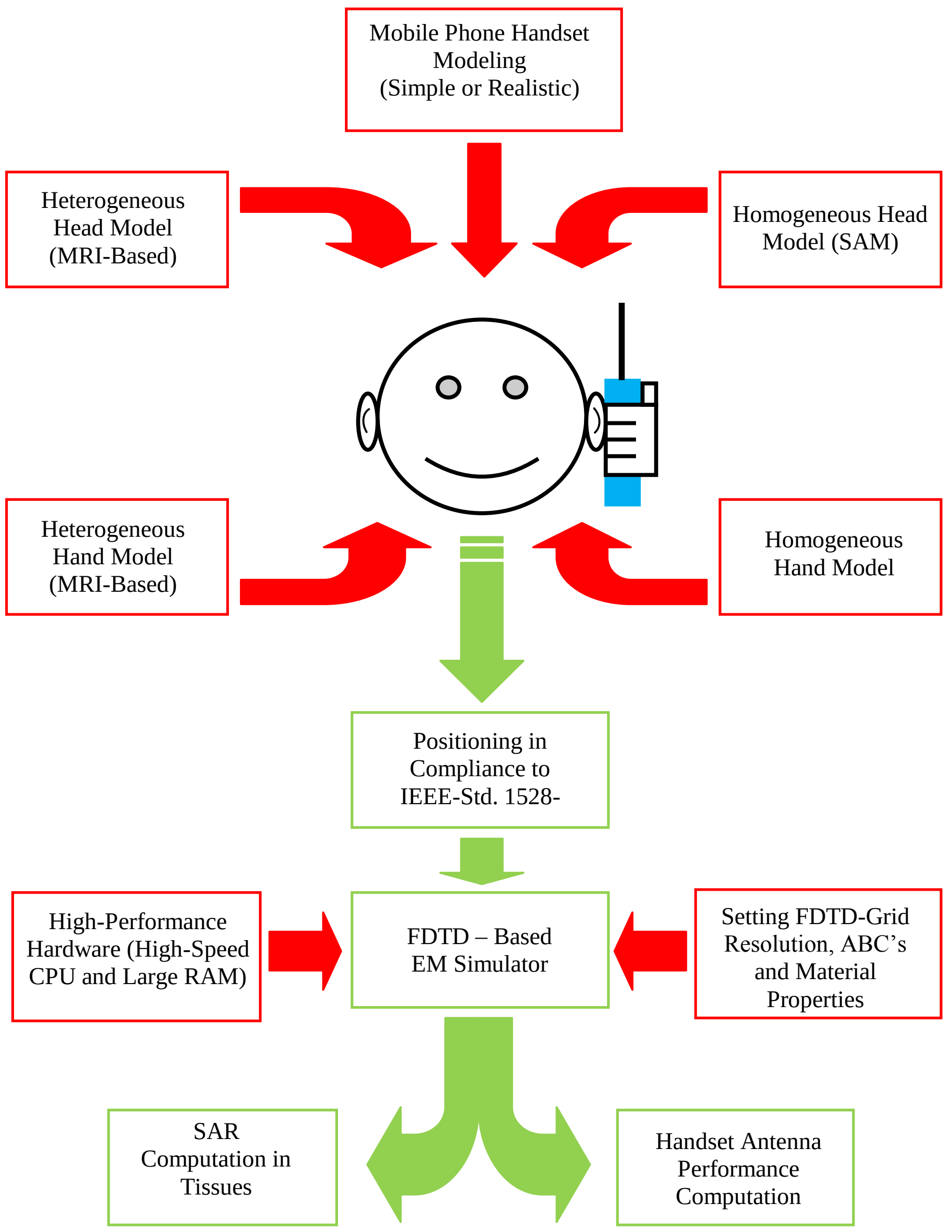

Figure 3. A block diagram illustrating the numerical computation of the EM interaction of a cellular handset and human using FDTD method.

Table 2. The generated FDTD-grid cell size of the generic phone in close proximity to SAM at *cheek* and *tilt* positions.

Frequency	*Cheek*-position	*Tilt*-position
835 MHz	$225 \times 173 \times 219 = 8.52458$ Mcells	$225 \times 170 \times 223 = 8.52975$ Mcells
1900 MHz	$191 \times 139 \times 186 = 4.93811$ Mcells	$191 \times 136 \times 186 = 4.83154$ Mcells

Table 3. Pooled SAR statistics that given in [26] and our computation, for the generic phone in close proximity to the SAM at *cheek* and *tilt*-position and normalized to 1 W input power.

Frequency			835 MHz		1900 MHz	
Handset position			*Cheek*	*Tilt*	*Cheek*	*Tilt*
FDTD Computation in literature [26]	Spatial-peak SAR_{1g} (W/kg)	Mean	7.74	4.93	8.28	11.97
		Std. Dev.	0.40	0.64	1.58	3.10
		No.	16	16	16	15
	Spatial-peak SAR_{10g} (W/kg)	Mean	5.26	3.39	4.79	6.78
		Std. Dev.	0.27	0.26	0.73	1.37
		No.	16	16	16	15
Measurement in literature [26]	Spatial-peak SAR_{1g} (W/kg)		8.8	4.8	8.6	12.3
	Spatial-peak SAR_{10g} (W/kg)		6.1	3.2	5.3	6.9
Our FDTD Computation	Spatial-peak SAR_{1g} (W/kg)		7.5	4.813	8.1	12.28
	Spatial-peak SAR_{10g} (W/kg)		5.28	3.13	4.36	6.51
Our ADI-FDTD Computation	Spatial-peak SAR_{1g} (W/kg)		7.44	4.76	8.2	12.98
	Spatial-peak SAR_{10g} (W/kg)		5.26	3.09	4.46	6.72

Figure 4 compares graphically the computation results of SAR over 1 and 10g in [26] with our computed using Yee-FDTD and ADI-FDTD methods, The computation results of both methods, i.e., Yee-FDTD and ADI-FDTD methods, showed a good agreement with that computed in [26]. When using the ADI-FDTD method, an ADI time step factor of 10 was set during simulation. The minimum value of the time step factor was 1 and increasing this value made the simulation run faster. With a time step factor ≥12, the speed of simulation will be faster than Yee-FDTD method [25]. Two solver optimizations are used: firstly, optimization for speed, where the ADI factorizations of tridiogonal systems performed at each iteration and a huge memory were needed, and secondly, optimization for memory, where the ADI factorizations of tridiogonal systems performed at each iteration took a long run-time.

The hardware used for simulation (Dell

Desk-Top, M1600, 1.6 GHz Dual Core, 4 GB DDRAM) was incapable of achieving optimization for speed while processing the generated grid-cells Mcells, and was also incapable of achieving optimization for memory while processing the generated grid-cellsMcells. When using the Yee-FDTD method, however, the hardware could process up to 22 Mcells [6]. No hardware accelerator such as an Xware [25] was used in the simulations.

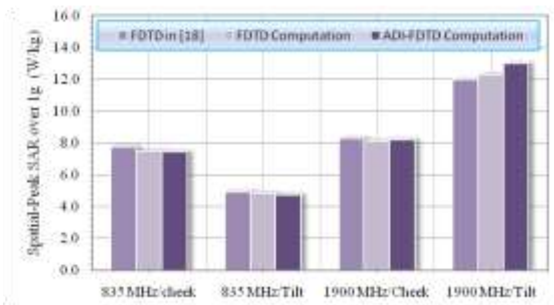

(a)

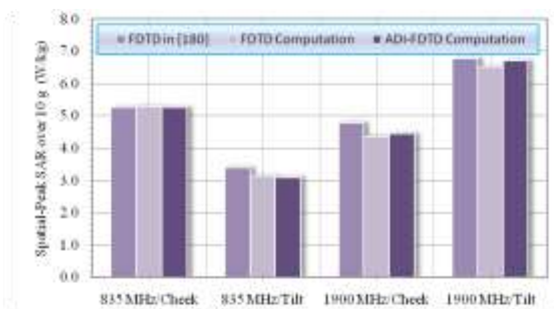

(b)

Figure 4. Spatial-peak SAR (IEEE-Std. 1529) computed in [26], computed using FDTD method and computed using ADI-FDTD method: (a) averaged over 1g, and (b) averaged over 10g. The results are normalized to net input power of 1 W.

7 FACTORS INFLUENCING THE EM INTERACTION

The EM wave interaction between the mobile phone handset and human head has been reported in many papers. Studies concentrated firstly, on the effect of the human head on the handset antenna performance, including the feed-point impedance, gain, and efficiency [36]-[39], and secondly, on the impact of the antenna EM radiation on the user's head, caused by the absorbed power, and measured by predicting the induced specific absorption rate (SAR) in the head tissues [1]-[3], [40]-[54]. During realistic usage of cellular handsets, many factors may play an important role by increasing or decreasing the EM interaction between the handset antenna and the user's head. The factors influencing the interaction include:

(a) **PCB and antenna positions** [7]; A hand-set model (generic mobile phone) formed by a monopole antenna and a PDB embedded in a chassis, with the excitation point at the base of the antenna, is simulated using FDTD-based EM-solver. Two cases were considered during the simulation; the first was varying the antenna+PCB position along the y-axis (chassis depth) with 9-steps, the second; was varying the antenna along the x-axis (chassis width) with 11-steps and keeping the PCB in the middle. The results showed that the optimum position for the antenna and PCB in hand-set close to head is the far right-corner for the right-hand users and the far left-corner for the left-hand users, where a minimum SAR in head is achieved.

(b) **Cellular handset shape** [4]; A novel cellular handset with a keypad over the screen and a bottom-mounted antenna has been proposed and numerically modeled, with the most handset components, using an FDTD-based EM solver. The proposed handset model is based on the commercially available model with a top-mounted external antenna. Both homogeneous and nonhomogeneous head phantoms have been used with a semirealistic hand design to simulate the handset in hand close to head. The simulation results showed a significant improvement in the antenna performance with the proposed handset model in hand close to head, as compared with the handset of top-mounted antenna. Also, using this proposed handset, a significant reduction in the induced SAR and power absorbed in head has been achieved.

(c) **Cellular handset position with respect to head** [8]; Both the computation accuracy and the cost were investigated in terms of the number of FDTD-grid cells due to the artifact rotation for a cellular handset close to the user's head. Two study cases were simulated to assess the EM coupling of a cellular handset and a MRI-based human head model at 900 MHz; firstly, both handset and head CAD models are aligned to the FDTD-grid, secondly, handset close to a rotated head in compliance with IEEE-1528 standard. A FDTD-based platform, SEMCAD X, is used; where conventional and interactive gridder approaches are implemented to achieve the simulations. The results show that owing to the artifact rotation, the computation error may increase up to 30%, whereas, the required number of grid cells may increase up to 25%.

(d) **Human head of different originations** [11]; Four homogeneous head phantoms of different human origins, i.e., African female, European male, European old male, and Latin American male, with normal (non-pressed) ears are designed and used in simulations for evaluating the electromagnetic (EM) wave interaction between handset antennas and human head at 900 and 1800MHz with radiated power of 0.25 and 0.125 W, respectively. The difference in heads dimensions due to different origins shows different EM wave interaction. In general, the African female's head phantom showed a higher induced SAR at 900 MHz and a lower induced SAR at 1800 MHz, as compared with the other head phantoms. The African female's head phantom also showed more impact on both mobile phone models at 900 and 1800 MHz. This is due to the different pinna size and thickness that every adopted head phantom had, which made the distance between the antenna source and nearest head tissue of every head phantom was different accordingly

(e) **hand-hold position, Antenna type, and human head model type [5],** [6]; For a realistic usage pattern of mobile phone handset, i.e., *cheek* and *tilt*-positions, with an MRI-based human head model and semi-realistic mobile phone of different types, i.e., candy-bar and clamshell types with external and internal antenna, operating at GSM-900, GSM-1800, and UMTS frequencies, the following were observed; handhold position had a considerable impact on handset antenna matching, antenna radiation efficiency, and TIS. This impact, however, varied due to many factors, including antenna type/position, handset position in relation to head, and operating frequency, and can be summarized as follows:

1. The significant degradation in mobile phone antenna performance was noticed for the candy-bar with patch antenna. This is because the patch antenna is sandwiched between hand and head tissues during use, and the hand tissues acted as the antenna upper dielectric layers. This may shift the tuning frequency as well as decrease the radiation efficiency.
2. Owing to the hand-hold alteration in different positions, the internal antenna of candybar-type handsets exhibited more variation in total efficiency values than the external antenna. The maximum absolute difference (25%) was recorded at 900MHz for a candy-bar type handset with bottom patch antenna against HR-EFH at *tilt*-position.
3. Maximum TIS level was obtained for the candy-bar handheld against head at *cheek*-position operating at 1800 MHz, where a minimum total efficiency was recorded when simulating handsets with internal patch antenna.
4. There was more SAR variation in HR-EFH tissues owing to internal antenna exposure, as compared with external antenna exposure.

8 CONCLUSION

A procedure for evaluating the EM interaction between mobile phone antenna and human head using numerical techniques, e.g., FDTD, FE, MoM, has been presented in this paper. A validation of our EM interaction computation using both Yee-FDTD and ADI-FDTD was achieved by comparison with previously published papers. A review of the factors may affect on the EM interaction, e.g., antenna type, mobile handset type, antenna position, mobile handset position, etc., was demonstrated. It was shown that the mobile handset antenna specifications may affected dramatically due to the factors listed above, as well as, the amount of the SAR deposited in the human head may also changed dramatically due to the same factors.

ACKNOWLEDGEMENTS

The author would like to express his appreciation to Prof. Dr. **Cynthia Furse** at University of Utah, USA, for her technical advice and provision of important references. Special thanks are extended to reverent **Wayne Jennings** at Schmid & Partner Engineering AG (SPEAG), Zurich, Switzerland, for his kind assistance in providing the license for the SEMCAD platform and the numerical corrected model of a human head (HR-EFH). The author also grateful to Dr. **Theodoros Samaras** at the Radiocommunications Laboratory, Department of Physics, Aristotle University of Thessaloniki, Greece, to **Esra Neufeld** at the Foundation for Research on Information Technologies in Society (IT'IS), ETH Zurich, Switzerland, and to **Peter Futter** at SPEAG, Zurich, Switzerland, for their kind assistance and technical advices.

REFERENCES

1. Chavannes, N., Tay, R., Nikoloski, N., Kuster, N.: Suitability of FDTD-based TCAD tools for RF design of mobile phones. IEEE Antennas & Propagation Magazine, vol. 45, no. 6, pp. 52--66 (2003)

2. Chavannes, N., Futter, P., Tay, R., Pokovic, K., Kuster, N.: Reliable prediction of mobile phone performance for different daily usage patterns using the FDTD method. In: Proceedings of the IEEE International Workshop on Antenna Technology (IWAT '06), White Plains, pp. 345--348, NY, USA (2006)
3. Futter, P., Chavannes, N., Tay, R. et al.: Reliable prediction of mobile phone performance for realistic in-use conditions using the FDTD method. IEEE Antennas and Propagation Magazine, vol. 50, no. 1, pp. 87--96 (2008)
4. Al-Mously, S.I., Abousetta, M.M.: A Novel Cellular Handset Design for an Enhanced Antenna Performance and a Reduced SAR in the Human Head. International Journal of Antennas and Propagation (IJAP), vol. 2008, Article ID 642572, 10 pages (2008)
5. Al-Mously, S.I., Abousetta, M.M.: A Study of the Hand-Hold Impact on the EM Interaction of A Cellular Handset and A Human Head. International Journal of Electronics, Circuits, and Systems (IJECS), vol. 2, no. 2, pp. 91--95 (2008)
6. Al-Mously, S.I., Abousetta, M.M.: Anticipated Impact of Hand-Hold Position on the Electromagnetic Interaction of Different Antenna Types/Positions and a Human in Cellular Communications. International Journal of Antennas and Propagation (IJAP), vol. 2008, 22 pages (2008)
7. Al-Mously, S.I., Abousetta, M.M.: Study of Both Antenna and PCB Positions Effect on the Coupling Between the Cellular Hand-Set and Human Head at GSM-900 Standard. In Proceeding of the International Workshop on Antenna Technology 2008, iWAT2008, pp. 514--517, Chiba, Japan (2008)
8. Al-Mously, S.I., Abdalla, A.Z., Abousetta, Ibrahim, E.M.: Accuracy and Cost Computation of the EM Coupling of a Cellular Handset and a Human Due to Artifact Rotation. In: Proceeding of 16th Telecommunication Forum TELFOR 2008, November 25-27, pp. 484--487, Belgrade, Serbia (2008)
9. Al-Mously, S.I., Abousetta, M.M.: User's Hand Effect on TIS of Different GSM900/1800 Mobile Phone Models Using FDTD Method. In: Proceeding of the International Conference on Computer, Electrical, and System Science, and Engineering, (The World Academy of Science, Engineering and Technology, PWASET), vo. 37, pp. 878--883, Dubai, UAE (2009)
10. Al-Mously, S.I., Abousetta, M.M.: Effect of the hand-hold position on the EM Interaction of clamshell-type handsets and a human. In: Proceeding of the Progress in Electromagnetics Research Symposium (PIERS), 18-21 August, pp. 1727--1731, Moscow, Russia (2009)
11. Al-Mously, S.I., Abousetta, M.M.: Impact of human head with different originations on the anticipated SAR in tissue. In: Proceeding of the Progress in Electromagnetics Research Symposium (PIERS), 18-21 August, pp. 1732--1736, Moscow, Russia (2009)
12. Al-Mously, S.I., and Abousetta, M.M.: A definition of thermophysiological parameters of SAM materials for temperature rise calculation in the head of cellular handset user. In Proceeding of the Progress in Electromagnetics Research Symposium (PIERS), 18-21 August, Moscow, Russia, pp. 170--174 (2009)
13. IEEE Recommended Practice for Determining the Peak Spatial-Average Specific Absorption Rate (SAR) in the Human Head from Wireless Communications Devices: Measurement Techniques, IEEE Standard-1528 (2003)
14. Allen, S.G.: Radiofrequency field measurements and hazard assessment. Journal of Radiological Protection, vol. 11, pp. 49--62 (1996)
15. Standard for Safety Levels with Respect to Human Exposure to Radiofrequency Electromagnetic Fields, 3 kHz to 300 GHz, IEEE Standards Coordinating Committee 28.4 (2006)
16. Product standard to demonstrate the compliance of mobile phones with the basic restrictions related to human exposure to electromagnetic fields (300 MHz–3GHz), European Committee for Electrical Standardization (CENELEC), EN 50360, Brussels (2001)
17. Basic Standard for the Measurement of Specific Absorption Rate Related to Exposure to Electromagnetic Fields from Mobile Phones (300 MHz–3GHz), European Committee for Electrical Standardization (CENELEC), EN-50361 (2001)

18. Human exposure to radio frequency fields from hand-held and body-mounted wireless communication devices - Human models, instrumentation, and procedures — Part 1: Procedure to determine the specific absorption rate (SAR) for hand-held devices used in close proximity to the ear (frequency range of 300 MHz to 3 GHz), IEC 62209-1 (2006)
19. Specific Absorption Rate (SAR) Estimation for Cellular Phone, Association of Radio Industries and businesses, ARIB STD-T56 (2002)
20. Evaluating Compliance with FCC Guidelines for Human Exposure to Radio Frequency Electromagnetic Field, Supplement C to OET Bulletin 65 (Edition 9701), Federal Communications Commission (FCC),Washington, DC, USA (1997)
21. ACA Radio communications (Electromagnetic Radiation - Human Exposure) Standard 2003, Schedules 1 and 2, Australian Communications Authority (2003)
22. Kuster, N., Balzano, Q.: Energy absorption mechanism by biological bodies in the near field of dipole antennas above 300 MHz. IEEE Transaction on Vehicular Technology, vol. 41, no. 1, Feb., pp. 17--23 (1992)
23. Caputa, K., Okoniewski, M., Stuchly, M. A.: An algorithm for computations of the power deposition in human tissue. IEEE Antennas and Propagation Magazine, vol. 41, pp. 102--107 (1999)
24. Recommended Practice for Determining the Peak Spatial-Average Specific Absorption Rate (SAR) associated with the use of wireless handsets - computational techniques, IEEE-1529, draft standard.
25. SEMCAD, Reference Manual for the SEMCAD Simulation Platform for Electromagnetic Compatibility, Antenna Design and Dosimetry, SPEAG-Schmid & Partner Engineering AG, http://www.semcad.com/.
26. Beard, B.B., Kainz, W., Onishi, T., et al.: Comparisons of computed mobile phone induced SAR in the SAM phantom to that in anatomically correct models of the human head. IEEE Transaction on Electromagnetic Compatibility, vol. 48, no. 2, pp. 397--407 (2006)
27. Procedure to measure the Specific Absorption Rate (SAR) in the frequency range of 300MHz to 3 GHz - part 1: handheld mobile wireless communication devices, International Electrotechnical Commission, committee draft for vote, IEC 62209.
28. ICNIRP, Guidelines for limiting exposure to time-varying electric, magnetic, and electromagnetic fields (up to 300 GHz), Health Phys., vol.74, no. 4, pp. 494--522 (1998)
29. Zombolas, C.: SAR Testing and Approval Requirements for Australia. In: Proceeding of the IEEE International Symposium on Electromagnetic Compatibility, vol. 1, pp. 273-278 (2003)
30. IEEE Standard for Safety Levels With Respect to Human Exposure to Radio Frequency Electromagnetic Fields, 3kHz to 300 GHz, Amendment2: Specific Absorption Rate (SAR) Limits for the Pinna, IEEE Standard C95.1b-2004 (2004)
31. Ghandi, O.P., and kang, G.: Inaccuracies of a plastic pinna SAM for SAR testing of cellular telephones against IEEE and ICNIRP safety guidelines. IEEE Transaction on Microwave Theory and Techniques, vol. 52, no. 8, (2004)
32. Ghandi, O.P., kang, G.: Some present problems and a proposed experimental phantom for SAR compliance testing of cellular telephones at 835 and 1900 MHz. Phys. Med. Biol., vol. 47, pp. 1501--1518 (2002)
33. Kuster, N., Christ, A., Chavannes, N., Nikoloski, N., Frolich, J.: Human head phantoms for compliance and communication performance testing of mobile telecommunication equipment at 900 MHz. In: Proceeding of the 2002 Interim Int. Symp. Antennas Propag., Yokosuka Research Park, Yokosuka, Japan (2002)
34. Christ, A., Chavannes, N., Nikoloski, N., Gerber, H., Pokovic, K., Kuster, N.: A numerical and experimental comparison of human head phantoms for compliance testing of mobile telephone equipment. Bioelectromagnetics, vol. 26, pp. 125--137 (2005)
35. Beard, B.B., Kainz, W.: Review and standardization of cell phone exposure calculations using the SAM phantom and anatomically correct head models. BioMedical Engineering Online 2004, 3:34, doi: 10.1186/1475-925X-3-34, (2004)

36. Kouveliotis, N.K., Panagiotou, S.C., Varlamos, P.K., Capsalis, C.N.: Theoretical approach of the interaction between a human head model and a mobile handset helical antenna using numerical methods. Progress In Electromagnetics Research, PIER 65, pp. 309–327 (2006)
37. Sulonen, K., Vainikainen, P.: Performance of mobile phone antennas including effect of environment using two methods. IEEE Transaction on Instrumentation and Measurement, vol. 52, no. 6, pp. 1859–1864 (2003)
38. Krogerus, J., Icheln, C., Vainikainen, P.: Dependence of mean effective gain of mobile terminal antennas on side of head. In: Proceedings of the 35th European Microwave Conference, pp. 467--470, Paris, France (2005)
39. Haider, H., Garn, H., Neubauer, G., Schmidt, G.: Investigation of mobile phone antennas with regard to power efficiency and radiation safety. In: Proceeding of the Workshop on Mobile Terminal and Human Body Interaction, Bergen, Norway (2000)
40. Toftgard, J., Hornsleth, S.N., Andersen, J.B.: Effects on portable antennas of the presence of a person: IEEE Transaction on Antennas and Propagation, vol. 41, no. 6, pp. 739--746 (1993)
41. Jensen, M.A., Rahmat-Samii, Y.: EM interaction of handset antennas and a human in personal communications. In: Proceeding of the IEEE, vol. 83, no. l, pp. 7-17 (1995)
42. Graffin, J., Rots, N., Pedersen, G. F.: Radiations phantom for handheld phones. In Proceedings of the IEEE Vehicular Technology Conference (VTC '00), vol. 2, pp. 853--860, Boston, Mass, USA (2000)
43. Khalatbari, S., Sardari, D., Mirzaee, A. A., Sadafi, H. A.: Calculating SAR in Two Models of the Human Head Exposed to Mobile Phones Radiations at 900 and 1800MHz. In: Proceedings of the Progress In Electromagnetics Research Symposium, pp. 104--109 Cambridge, USA, (2006)
44. Okoniewski, M., Stuchly, M.: A study of the handset antenna and human body interaction. IEEE Transaction on Microwave Theory and Techniques, vol. 44, no. 10, pp. 1855--1864 (1996)
45. Bernardi, P., Cavagnaro, M., Pisa, S.: Evaluation of the SAR distribution in the human head for cellular phones used in a partially closed environment. IEEE Transactions of Electromagnetic Compatibility, vol. 38, no. 3, pp. 357--366 (1996).
46. Lazzi, G., Pattnaik, S. S., Furse, C. M., Gandhi, O. P.: Comparison of FDTD computed and measured radiation patterns of commercial mobile telephones in presence of the human head. IEEE Transaction on Antennas and Propagation, vol. 46, no. 6, pp. 943--944 (1998)
47. Koulouridis S., Nikita, K. S.: Study of the coupling between human head and cellular phone helical antennas. IEEE Transactions of Electromagnetic Compatibility, vol. 46, no. 1, pp. 62--70 (2004)
48. Wang J., Fujiwara, O.: Comparison and evaluation of electromagnetic absorption characteristics in realistic human head models of adult and children for 900-MHz mobile telephones. IEEE Transactions on Microwave Theory and Techniques, vol. 51, no. 3, pp. 966--971 (2003)
49. Lazzi G., Gandhi, O.P.: Realistically tilted and truncated anatomically based models of the human head for dosimetry of mobile telephones. IEEE Transactions of Electromagnetic Compatibility, vol. 39, no. 1, pp. 55-61 (1997)
50. Rowley, J.T., Waterhouse, R.B.: Performance of shorted microstrip patch antennas for mobile communications handsets at 1800 MHz. IEEE Transaction on Antennas and Propagation, vol. 47, no. 5, pp. 815--822 (1999)
51. Watanabe, S.-I, Taki, M. Nojima, T., Fujiwara, O.: Characteristics of the SAR distributions in a head exposed to electromagnetic field radiated by a hand-held portable radio. IEEE Transaction on Microwave Theory and Techniques, vol. 44, no. 10, pp. 1874--1883 (1996)
52. Bernardi, P., Cavagnaro, M., Pisa, S., Piuzzi, E.: Specific absorption rate and temperature increases in the head of a cellular-phone user. IEEE Transaction on Microwave Theory and Techniques, vol. 48, no. 7, pp. 1118--1126 (2000)
53. Lee, H., Choi, Lee H., Pack, J.: Human head size and SAR characteristics for handset exposure. ETRI Journal, vol. 24, pp. 176-179 (2002)
54. Francavilla, M., Schiavoni, A., Bertotto, P., Richiardi, G.: Effect of the hand on cellular phone radiation. IEE Proceeding of Microwaves, Antennas and Propagation, vol. 148, pp. 247--253 (2001)